TRAJECTORY TRACKING CONTROL FOR OFFSHORE BOOM CRANES USING HIGHER-ORDER SLIDING MODES

*R. M. T. Raja Ismail and Q. P. Ha
Faculty of Engineering and IT, University of Technology Sydney
15 Broadway
NSW 2007, Australia
*(*Corresponding author: raja.rajaismail@uts.edu.au)*

TRAJECTORY TRACKING CONTROL FOR OFFSHORE BOOM CRANES USING HIGHER-ORDER SLIDING MODES

ABSTRACT

Shipping and stevedoring industry is going to witness a massive increase in the amount of containers to be handled while land constraints become more critical. Offshore transfer operations hence offer a preferable solution to deal with the surge in cargos rather than to expand the port outwards. Recently, there has been increasing research interests on offshore crane automation. Suspended cargos in a ship-mounted crane system are caused to swing due to the vibratory motion of the ship induced by ocean waves, which can lead to collision between cargos and deck. Therefore, it is vital for offshore crane systems to satisfy rigorous requirements in terms of safety and efficiency. This paper presents the modelling and control development for offshore boom crane systems. A second-order sliding mode control law is proposed for trajectory tracking and sway suppression control, making use of its capability of actuator chattering alleviation while achieving high tracking performance and preserving strong robustness. The asymptotic stability of the closed-loop system is guaranteed in the Lyapunov sense. Simulation results indicate that the proposed controller can significantly reduce the effect of disturbances coming from gusty waves and other dynamic loadings.

KEYWORDS

Offshore boom crane automation, Second-order sliding mode, Lyapunov stability

INTRODUCTION

One of the fastest growing segments of the world shipping industry is that of containers. It has been reported that the level of container traffic through major ports in America, Europe and Asia has increases significantly in recent years (González & Trujillo, 2008; Goodchild & Daganzo, 2007; Low et al., 2009). In response to growth in demand, increased ship sizes and competition, there has also been near simultaneous ambitions for many ports to pursue expansion (Fan et al, 2012). However, expanding outwards is not a feasible solution due to land constraints. As a result, they are examining alternative ways to cope with the potential surge in cargo handling demands (Yin et al., 2011). One way to improve port efficiency is open-sea ship-to-ship transfer operations, which involve the transfer of containers between seagoing ships positioned alongside each other, either while stationary or underway, as shown in Figure 1. As a result, port congestion due to the increased of cargo ships traffic can be minimized.

Research on cranes' control and automation has focused on addressing challenges in their offshore operations (Küchler et al., 2011; Messineo & Serrani, 2009; Skaare & Egeland, 2006). The synthesis of feedback control for offshore cranes remains a challenge since the systems involve the presence of parameter variations, e.g. changes of load during the process of loading/unloading, and the presence of disturbances, e.g. wave- and wind-induced movements. Besides, the presence of obstacles around the environment, such as harbour and vessel, must be taken into consideration for the path planning of load transportation. The models and control strategies of the gantry-type and boom-type offshore cranes have been reported in Ngo & Hong (2012) and Fang & Wang (2012), respectively. However, obtaining the offshore crane models which reflect their real motions and environment, and synthesizing the control algorithms remains a challenge due to a large number of degrees-of-freedom must be taken into consideration in developing the cranes' dynamics.

Sliding mode control offers a good capability to deal with uncertainties and nonlinearities of a plant. The methodology is based on keeping exactly a properly chosen dynamic constraint by means of high-frequency control switching, and is known as robust and very accurate. The first-order sliding mode control (1-SMC) has been successfully implemented in surface vessel and offshore crane systems (Ashrafiuon, 2008; Fahimi, 2007; Ngo & Hong, 2012; Yu et al., 2012). Unfortunately, 1-SMC general application may be restricted, i.e., for an output sliding function to be zeroed, the standard sliding mode may keep the sliding function equal to zero only if the outputs relative degree is one (Levant, 2007). High-frequency control switching may also cause the undesired chattering effect (Boiko et al., 2010). Higher-order sliding modes remove the relative degree restriction and, if properly designed, can practically eliminate the chattering. A few numbers of papers have addressed the application of second-order sliding mode control (2-SMC) in crane automations. The implementations of second-order sliding mode controller and observer for laboratory gantry cranes control have been reported in Bartolini et al. (2002) and Raja Ismail et al. (2012). The development of 2-SMC for gantry type offshore crane has also been reported in Raja Ismail & Ha (2012).

This paper presents the modelling and control development for offshore boom cranes system. A second-order sliding mode control (2-SMC) law is proposed for trajectory tracking and sway suppression control, making use of its capability of actuator chattering alleviation while achieving high tracking performance and preserving strong robustness. The asymptotic stability of the closed-loop system is guaranteed in the Lyapunov sense. Simulation results indicate that the proposed controller can significantly reduce the effect of disturbances coming from gusty waves and other dynamic loadings.

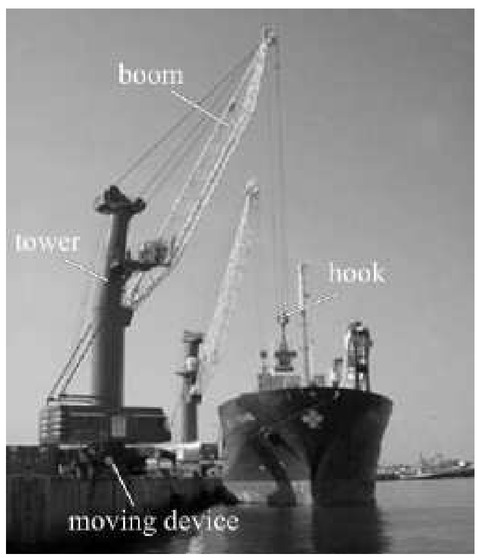

Figure 1 – Offshore boom crane (Neupert et al., 2006)

MODELLING OF OFFSHORE BOOM CRANES

The offshore crane system considered in this study consists of a boom crane mounted on a ship vessel. The coordinates system of the offshore crane is shown in Figure 2, where $\{o_N x_N y_N z_N\}$ and $\{o_B x_B y_B z_B\}$ are respectively represent the coordinate frames of the ground and the vessel. The masses of the boom and the payload are respectively denoted by m_b and m. The lengths L_b and l are respectively for the boom and the rope, and h is the height of the tower. θ is the luff angle of the boom, ϕ is the swing angle of the payload and ψ is the roll angle of the vessel due to the ocean wave. Thus, the dynamic model of the offshore crane system can be cast in the form of

$$\mathbf{D}(\mathbf{q})\ddot{\mathbf{q}} + \mathbf{C}(\mathbf{q},\dot{\mathbf{q}})\dot{\mathbf{q}} + \mathbf{B}\dot{\mathbf{q}} + \mathbf{G}(\mathbf{q}) = \boldsymbol{\tau}\,, \tag{1}$$

where $\mathbf{D}(\mathbf{q})$ is the inertia, $\mathbf{C}(\mathbf{q},\dot{\mathbf{q}})$ is the centrifugal-Coriolis, $\mathbf{B}$ is the friction, and $\mathbf{G}(\mathbf{q})$ is the gravity matrices.

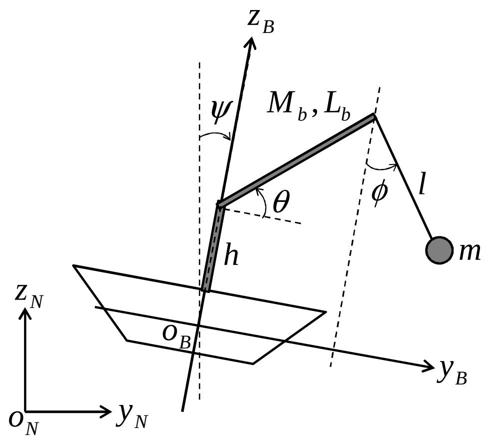

Figure 2 – Motion of the offshore boom crane system

The system matrices are defined as follows:

$$\mathbf{D}(\mathbf{q})=\begin{bmatrix} \frac{1}{12}M_b(4L_b^2+w_b^2)+m[L_b^2+2l^2-2L_bl\sin(\theta-\phi)] & -mL_b\cos(\theta-\phi) & m[2l^2-L_bl\sin(\theta-\phi)] \\ -mL_b\cos(\theta-\phi) & m & 0 \\ m[2l^2-L_bl\sin(\theta-\phi)] & 0 & 2ml^2 \end{bmatrix},$$

$$\mathbf{C}(\mathbf{q},\dot{\mathbf{q}})=\begin{bmatrix} m[-L_bl\cos(\theta-\phi)(\dot\theta-\dot\phi)-L_b\dot l\sin(\theta-\phi)+2l\dot l] & m[-L_bl\sin(\theta-\phi)\dot\phi+2l\dot\phi] & m[L_bl\cos(\theta-\phi)\dot\phi-L_b\dot l\sin(\theta-\phi)+2l\dot l] \\ m[L_b\sin(\theta-\phi)\dot\theta-2l\dot\phi] & 0 & -2ml\dot\phi \\ m[-L_bl\cos(\theta-\phi)\dot\theta+2l\dot l] & 2ml\dot\phi & 2ml\dot l \end{bmatrix},$$

$$\mathbf{B}=\mathrm{diag}(B_\theta,B_l,B_\phi), \qquad \mathbf{G}(\mathbf{q})=\left[\tfrac{1}{2}M_bgL_b\cos\theta+mg(L_b\cos\theta+l\sin\phi) \quad -mg\cos\phi \quad mgl\sin\phi\right]^T,$$

where g is the gravitational acceleration. The vector of generalized coordinates $\mathbf{q}$ and the input vector $\boldsymbol{\tau}$ are respectively defined as $\mathbf{q}=[\theta,l,\phi]^T$ and $\boldsymbol{\tau}=[\tau_b, f_l, 0]^T$.

In order to find the payload swing angle with respect to the ground coordinate frame, at first we obtain the position vector $\mathbf{p}_m$ of the payload with respect to the vessel coordinate frame $\{o_Bx_By_Bz_B\}$ as

$$\mathbf{p}_m=[x_m,y_m,z_m]^T=[0,\ L_b\cos\theta+l\sin\theta,\ h+L_b\sin\theta-l\cos\theta]^T.$$

The position vector of the payload coordinates with respect to the ground coordinate frame $\{o_Nx_Ny_Nz_N\}$, namely $\mathbf{p}'_m$, can be obtained by multiplying the augmented position vector of $\mathbf{p}_m$ with the homogenous transformation matrix

$$\mathrm{T}_N^B = \begin{bmatrix} 1 & 0 & 0 & 0 \\ 0 & 1 & -\sin\psi & 0 \\ 0 & \sin\psi & \cos\psi & z \\ 0 & 0 & 0 & 1 \end{bmatrix},$$

such that $\mathbf{P}'_m = [x'_m, y'_m, z'_m, 1]^T = \mathrm{T}_N^B \mathbf{P}_m$, where ψ and z are respectively the roll and the heave of the vessel, while $\mathbf{P}_m = [\mathbf{p}_m^T, 1]^T$ and $\mathbf{P}'_m = [\mathbf{p}'^T_m, 1]^T$ are the augmented vectors of homogenous representation. Therefore, the payload swing angle with respect to the ground coordinate frame $\{o_N x_N y_N z_N\}$, namely δ, is defined as

$$\delta = \phi - \psi = \tan^{-1}\left[\frac{y'_m - h\sin\psi - L_b\cos(\theta-\psi)}{-z'_m + z + h\cos\psi + L_b\sin(\theta-\psi)}\right].$$

SECOND-ORDER SLIDING MODE CONTROL

This section presents the design of the control algorithm for trajectory tracking control of the offshore crane.

The Control Algorithm

The vectors of generalized coordinates can be partitioned as $\mathbf{q}^T = [\mathbf{q}_a^T, \mathbf{q}_u^T]$ where $\mathbf{q}_a$ and $\mathbf{q}_u$ are the actuated and underactuated state vectors respectively. Similarly we partition the input vector as $\boldsymbol{\tau}^T = [\mathbf{u}^T, 0^T]$. The partitioned vectors are defined as follows:

$$\mathbf{q}_a = [\theta, l]^T, \quad \mathbf{q}_u = \phi, \quad \mathbf{u} = [\tau_b, f_l]^T.$$

Then (1) can be rewritten as

$$\begin{bmatrix} \mathbf{D}_{aa}(\mathbf{q}) & \mathbf{D}_{au}(\mathbf{q}) \\ \mathbf{D}_{ua}(\mathbf{q}) & \mathbf{D}_{uu}(\mathbf{q}) \end{bmatrix}\begin{bmatrix} \ddot{\mathbf{q}}_a \\ \ddot{\mathbf{q}}_u \end{bmatrix} + \begin{bmatrix} \mathbf{C}_{aa}(\mathbf{q},\dot{\mathbf{q}}) & \mathbf{C}_{au}(\mathbf{q},\dot{\mathbf{q}}) \\ \mathbf{C}_{ua}(\mathbf{q},\dot{\mathbf{q}}) & \mathbf{C}_{uu}(\mathbf{q},\dot{\mathbf{q}}) \end{bmatrix}\begin{bmatrix} \dot{\mathbf{q}}_a \\ \dot{\mathbf{q}}_u \end{bmatrix} + \begin{bmatrix} \mathbf{B}_a & 0 \\ 0 & \mathbf{B}_u \end{bmatrix}\begin{bmatrix} \dot{\mathbf{q}}_a \\ \dot{\mathbf{q}}_u \end{bmatrix} + \begin{bmatrix} \mathbf{G}_a(\mathbf{q}) \\ \mathbf{G}_u(\mathbf{q}) \end{bmatrix} = \begin{bmatrix} \mathbf{u} \\ 0 \end{bmatrix}. \tag{2}$$

By substituting $\ddot{\mathbf{q}}_u = -\mathbf{D}_{uu}^{-1}(\mathbf{D}_{ua}\ddot{\mathbf{q}}_a + \mathbf{C}_{ua}\dot{\mathbf{q}}_a + \mathbf{C}_{uu}\dot{\mathbf{q}}_u + \mathbf{B}_u\dot{\mathbf{q}}_u + \mathbf{G}_u)$ obtained from the second row of (2) into the first row, we get the following form

$$\overline{\mathbf{D}}\ddot{\mathbf{q}}_a + \overline{\mathbf{C}}\dot{\mathbf{q}}_a + \mathbf{B}_a\dot{\mathbf{q}}_a + \overline{\mathbf{G}} + \mathbf{f}(\mathbf{q},\dot{\mathbf{q}}) = \mathbf{u}, \tag{3}$$

where $\overline{\mathbf{D}} = \mathbf{D}_{aa} - \mathbf{D}_{au}\mathbf{D}_{uu}^{-1}\mathbf{D}_{ua}$, $\overline{\mathbf{C}} = \mathbf{C}_{aa} - \mathbf{D}_{au}\mathbf{D}_{uu}^{-1}\mathbf{C}_{ua}$, $\overline{\mathbf{G}} = \mathbf{G}_a - \mathbf{D}_{au}\mathbf{D}_{uu}^{-1}\mathbf{G}_u$ and $\mathbf{f}(\mathbf{q},\dot{\mathbf{q}}) = (\mathbf{C}_{au} - \mathbf{D}_{au}\mathbf{D}_{uu}^{-1}\mathbf{C}_{uu})\dot{\mathbf{q}}_u - \mathbf{D}_{au}\mathbf{D}_{uu}^{-1}\mathbf{B}_u\dot{\mathbf{q}}_u$.

The tracking problem is constituted in finding a control action guaranteeing that $\lim_{t\to\infty}\mathbf{q}(t) = \mathbf{q}^d(t)$, where $\mathbf{q}^d(t)$ represents the reference trajectories for the vectors of generalized coordinates. By defining the tracking error as $\mathbf{e} = \mathbf{q} - \mathbf{q}^d$, similarly, it can be partitioned as $\mathbf{e}^T = [\mathbf{e}_a^T, \mathbf{e}_u^T]$, where

$$\mathbf{e}_a = [\theta - \theta^d, l - l^d]^T, \quad \mathbf{e}_u = \phi - \psi = \delta,$$

in which $\mathbf{e}_a(t)$ and $\mathbf{e}_u(t)$ are the tracking error vectors of the actuated and underactuated generalized coordinates.

Let us define the vector of sliding functions as

$$\boldsymbol{\sigma} = \begin{bmatrix} \sigma_1 \\ \sigma_2 \end{bmatrix} = \begin{bmatrix} \dot{\theta} - \dot{\theta}^d + \lambda_1(\theta - \theta^d) + \gamma\dot{\delta} + \lambda_3\delta \\ \dot{l} - \dot{l}^d + \lambda_2(l - l^d) \end{bmatrix},$$

or in a more convenient form

$$\boldsymbol{\sigma} = \dot{\mathbf{q}}_a - \dot{\mathbf{q}}_a^r, \tag{4}$$

where

$$\dot{\mathbf{q}}_a^r = \dot{\mathbf{q}}_a^d - \Lambda_a(\mathbf{q}_a - \mathbf{q}_a^d) - \Gamma\dot{\delta} - \Lambda_u\delta,$$

in which $\Lambda_a = \operatorname{diag}(\lambda_1, \lambda_2)$, $\Lambda_u = [\lambda_3, 0]^T$ and $\Gamma = [\gamma, 0]^T$. Thus, from (4) the second-order derivative of the sliding function is

$$\ddot{\boldsymbol{\sigma}} = \xi(\mathbf{q}, \dot{\mathbf{q}}, \mathbf{u}) + \overline{\mathbf{D}}^{-1}(\mathbf{q})\dot{\mathbf{u}},$$

where $\xi(\mathbf{q}, \dot{\mathbf{q}}, \mathbf{u}) = -\overline{\mathbf{D}}^{-1}(\mathbf{q})[\dot{\overline{\mathbf{D}}}(\mathbf{q})\ddot{\mathbf{q}}_a + \dot{\overline{\mathbf{C}}}(\mathbf{q}, \dot{\mathbf{q}})\dot{\mathbf{q}}_a + \overline{\mathbf{C}}(\mathbf{q}, \dot{\mathbf{q}})\ddot{\mathbf{q}}_a + \dot{\overline{\mathbf{G}}}(\mathbf{q}, \dot{\mathbf{q}}) + \dot{\mathbf{f}}(\mathbf{q}, \dot{\mathbf{q}})] - \ddot{\mathbf{q}}_a^r$. It is assumed here that the second-order derivative of the sliding function is bounded by a known function, i.e. $|\ddot{\sigma}_i| \leq \Upsilon_i(\cdot)$ (Pisano & Usai, 2011). In order to simplify the control synthesis, a constant value Υ_{Mi} is further assumed to exist such that $|\Upsilon_i(\cdot)| \leq \Upsilon_{Mi}$.

Consider an auxiliary system constituted by a double integrator with output $\mathbf{x}_1$ and input $\mathbf{w}$ defined as

$$\begin{aligned} \dot{\mathbf{x}}_1 &= \mathbf{x}_2 \\ \dot{\mathbf{x}}_2 &= \mathbf{w}. \end{aligned} \tag{5}$$

Putting $\boldsymbol{\varepsilon}_1 = \boldsymbol{\sigma} - \mathbf{x}_1$ yields

$$\begin{aligned} \dot{\boldsymbol{\varepsilon}}_1 &= \boldsymbol{\varepsilon}_2 \\ \dot{\boldsymbol{\varepsilon}}_2 &= \ddot{\boldsymbol{\sigma}} - \mathbf{w}, \end{aligned}$$

where $\boldsymbol{\varepsilon}_1$ is assumed bounded such that $|\varepsilon_{1i}| \leq \varepsilon_{1iM}$. The equivalent control of the system (5) can be obtained once the second-order sliding mode has been established on the manifold $\boldsymbol{\varepsilon}_1 = \boldsymbol{\varepsilon}_2 = 0$, i.e. $\mathbf{w}_{\mathrm{eq}} = \ddot{\boldsymbol{\sigma}} = \xi(\mathbf{q}, \dot{\mathbf{q}}, \mathbf{u}) + \overline{\mathbf{D}}^{-1}(\mathbf{q})\dot{\mathbf{u}}$. This leads to the equivalent representation of system (5) as follows:

$$\begin{aligned} \dot{\mathbf{x}}_1 &= \mathbf{x}_2 \\ \dot{\mathbf{x}}_2 &= \mathbf{w}_{\mathrm{eq}} = \ddot{\boldsymbol{\sigma}} = \xi(\mathbf{q}, \dot{\mathbf{q}}, \mathbf{u}) + \overline{\mathbf{D}}^{-1}(\mathbf{q})\dot{\mathbf{u}}. \end{aligned} \tag{6}$$

The equivalent system (6) can be stabilized by using first-order sliding mode control. Let us define the sliding function as

$$\mathbf{s} = \mathbf{x}_2 + \Lambda_x\mathbf{x}_1, \tag{7}$$

where Λ_x = diag(λ_{x1}, λ_{x2}). By defining the suitable discontinuous control $\dot{\mathbf{u}}$, the system (6) can be steered onto the sliding manifold $\mathbf{s} = 0$.

The proposed control algorithms for the control derivative $\dot{\mathbf{u}}$ and the auxiliary control signal $\mathbf{w}$ are defined as

$$\begin{aligned} \dot{u}_i &= -(\Xi_{M_i} + \eta_i)\,\mathrm{sign}\, s_i \\ w_i &= (2\Upsilon_{M_i} + \eta_i)\,\mathrm{sign}\left(\varepsilon_{1i} - \tfrac{1}{2}\varepsilon_{1i_M}\right),\ i = 1,2\ , \end{aligned} \tag{8}$$

where η_i is a positive constant and the definition of constant Ξ_{Mi} will be discussed in the next subsection.

Stability of the Equivalent System

From the condition $\boldsymbol{\varepsilon}_1 = \boldsymbol{\varepsilon}_2 = 0$ for the equivalent dynamics, we have

$$\begin{cases} \mathbf{x}_1 = \boldsymbol{\sigma} = \dot{\mathbf{q}}_a - \dot{\mathbf{q}}_a^r \\ \mathbf{x}_2 = \dot{\boldsymbol{\sigma}} = \ddot{\mathbf{q}}_a - \ddot{\mathbf{q}}_a^r \\ \ddot{\mathbf{q}}_a = \mathbf{s} - \Lambda_x \boldsymbol{\sigma} + \ddot{\mathbf{q}}_a^r. \end{cases} \tag{9}$$

To prove the stability of the equivalent system by means of control algorithm (8), we choose the following Lyapunov function candidate

$$V = \tfrac{1}{2}\mathbf{s}^T \overline{\mathbf{D}}\mathbf{s}\,.$$

Then, the derivative of V is

$$\dot{V} = \tfrac{1}{2}(\dot{\mathbf{s}}^T \overline{\mathbf{D}}\mathbf{s} + \mathbf{s}^T \dot{\overline{\mathbf{D}}}\mathbf{s} + \mathbf{s}^T \overline{\mathbf{D}}\dot{\mathbf{s}}) = \mathbf{s}^T \overline{\mathbf{D}}\dot{\mathbf{s}} + \tfrac{1}{2}\mathbf{s}^T \dot{\overline{\mathbf{D}}}\mathbf{s}\ .$$

From (4), (6) and (7), one has

$$\dot{\mathbf{s}} = \dot{\mathbf{x}}_2 + \Lambda_x \dot{\mathbf{x}}_1 = \ddot{\boldsymbol{\sigma}} + \Lambda_x \mathbf{x}_2 = \dddot{\mathbf{q}}_a - \dddot{\mathbf{q}}_a^r + \Lambda_x \mathbf{x}_2\ .$$

Thus,

$$\dot{V} = \mathbf{s}^T(\overline{\mathbf{D}}\dddot{\mathbf{q}}_a - \overline{\mathbf{D}}\dddot{\mathbf{q}}_a^r + \overline{\mathbf{D}}\Lambda_x \mathbf{x}_2) + \tfrac{1}{2}\mathbf{s}^T \dot{\overline{\mathbf{D}}}\mathbf{s}\ .$$

By differentiating (3), it can be shown that $\overline{\mathbf{D}}\dddot{\mathbf{q}}_a = -\dot{\overline{\mathbf{D}}}\ddot{\mathbf{q}}_a - \overline{\mathbf{C}}\ddot{\mathbf{q}}_a - \dot{\overline{\mathbf{C}}}\dot{\mathbf{q}}_a - \mathbf{B}_a\ddot{\mathbf{q}}_a - \dot{\overline{\mathbf{G}}} - \dot{\mathbf{f}}(\mathbf{q},\dot{\mathbf{q}}) + \dot{\mathbf{u}}$. Hence, from this equation and the last equation of (9), the derivative of the Lyapunov function becomes

$$\begin{aligned} \dot{V} &= \mathbf{s}^T[-\dot{\overline{\mathbf{D}}}\ddot{\mathbf{q}}_a - \overline{\mathbf{C}}\ddot{\mathbf{q}}_a - \dot{\overline{\mathbf{C}}}\dot{\mathbf{q}}_a - \mathbf{B}_a\ddot{\mathbf{q}}_a - \dot{\overline{\mathbf{G}}} - \dot{\mathbf{f}}(\mathbf{q},\dot{\mathbf{q}}) - \overline{\mathbf{D}}\dddot{\mathbf{q}}_a^r + \overline{\mathbf{D}}\Lambda_x\mathbf{x}_2 + \dot{\mathbf{u}}] + \tfrac{1}{2}\mathbf{s}^T\dot{\overline{\mathbf{D}}}\mathbf{s} \\ &= \mathbf{s}^T[-\dot{\overline{\mathbf{D}}}(\mathbf{s} - \Lambda_x\boldsymbol{\sigma} + \ddot{\mathbf{q}}_a^r) - \overline{\mathbf{C}}(-\Lambda_x\boldsymbol{\sigma} + \ddot{\mathbf{q}}_a^r) - \dot{\overline{\mathbf{C}}}\dot{\mathbf{q}}_a - \mathbf{B}_a\ddot{\mathbf{q}}_a - \dot{\overline{\mathbf{G}}} - \dot{\mathbf{f}}(\mathbf{q},\dot{\mathbf{q}}) - \overline{\mathbf{D}}\dddot{\mathbf{q}}_a^r + \overline{\mathbf{D}}\Lambda_x\mathbf{x}_2 + \dot{\mathbf{u}}] + \tfrac{1}{2}\mathbf{s}^T(\dot{\overline{\mathbf{D}}} - 2\overline{\mathbf{C}})\mathbf{s} \\ &= \mathbf{s}^T[\Xi(\mathbf{q},\dot{\mathbf{q}},\mathbf{u},\mathbf{q}_a^r,\dot{\mathbf{q}}_a^r,\ddot{\mathbf{q}}_a^r,\dddot{\mathbf{q}}_a^r) + \dot{\mathbf{u}}], \end{aligned}$$

given that the matrix $\dot{\overline{\mathbf{D}}} - 2\overline{\mathbf{C}}$ is skew-symmetric while all terms that do not contain the derivative of control signal $\dot{\mathbf{u}}$ are lumped into the function $\Xi(\cdot)$. To facilitate the proof, here if we define Ξ_{Mi} as the bound of this function, i.e., $|\Xi(\cdot)| \le \Xi_{Mi}$, then by substituting (8) into the last equation, it can be shown that

$$\dot{V} \le -\eta_i \mathbf{s}^T\mathbf{s}\,,$$

which implies that the surface $\mathbf{s} = 0$ is globally reached in finite time.

RESULTS AND DISCUSSION

In this study the values of the crane parameters are listed as M_b = 30×10^3 kg, m = 10×10^3 kg, h = 10 m, L_b = 21 m, w_b = 2.5 m, $\mathbf{B}$ = diag(0.1 N-m/rad-s^{-1},0.2 N/m-s^{-1},0.1 N-m/rad-s^{-1}), and g = 9.8065 ms^{-2}. The mobile harbour heave z and roll ψ are considered as disturbance, where z = 0.02 sin 1.25t m and ψ = 0.01 sin 1.25t rad. The controller parameters used in the simulations are $\lambda_1 = 2$, $\lambda_2 = \lambda_3 = 1$, $\gamma = 0.5$, $\lambda_{xi} = 1$, Ξ_{Mi} = 50×10^3, Υ_{Mi} = 10×10^3, η_i = 30 and ε_{1iM} = 10, $\forall i$ = 1, 2. The initial value of the generalized coordinates vector is chosen as (θ_0, l_0, ϕ_0) = (0 rad, 10 m, 0 rad). The swing angle response which will be presented in this section is the swing angle with respect to the ground coordinate frame δ, where $\delta = \phi - \psi$, as explained in the second section. The reference trajectories are chosen such that θ^d = 1.2 rad, l^d = 15 m, and $\delta^d = 0$ ($\phi^d = \psi$).

Several scenarios were considered for simulation to assess the capability of the proposed controller. The first one is by considering that the ship vessel is stationary, i.e. both its heave and roll are set to zero ($z = 0$ and $\psi = 0$) as shown in Figure 3. In this case, the swing angle is suppressed which results a small amplitude of oscillation after a few seconds the boom reached its reference luff angle, while the rope length reaches its reference after 5 seconds. The second scenario considered in the study is with the presence of both heave and pitch of the vessel as disturbances to the crane system, such that z = 0.02 sin 1.25t m and ψ = 0.01 sin 1.25t rad. In practical, this situation can occur due to the presence of ocean wave movements. As shown in Figure 4(b), the maximum amplitude of the swing angle increases to 0.03 rad due to the presence of disturbances. There are also relatively small oscillations in the luff angle and rope length responses as shown in Figures 4(a) and 4(c) respectively.

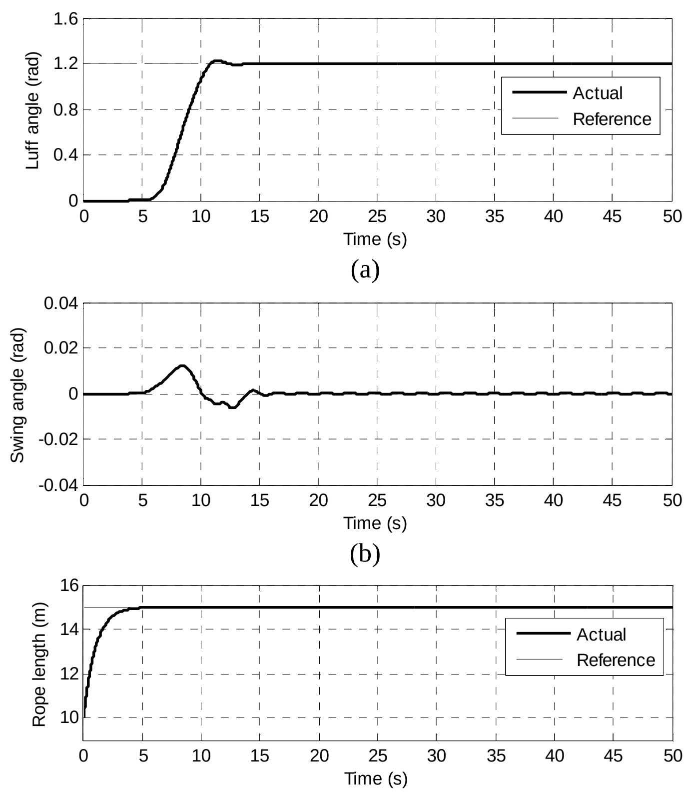

(a) (b) (c)

Figure 3 – (a) Luff angle; (b) swing angle; and (c) rope length; when the vessel is stationary, i.e. $z = 0$ and $\psi = 0$.

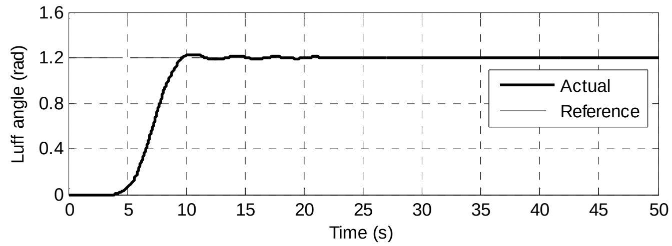

(a)

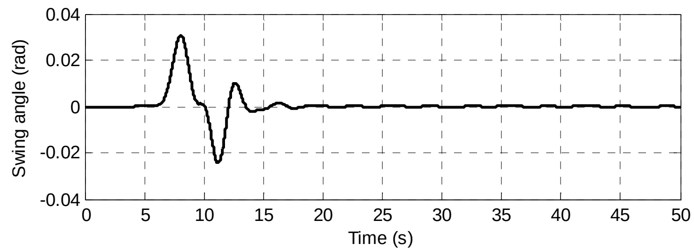

(b)

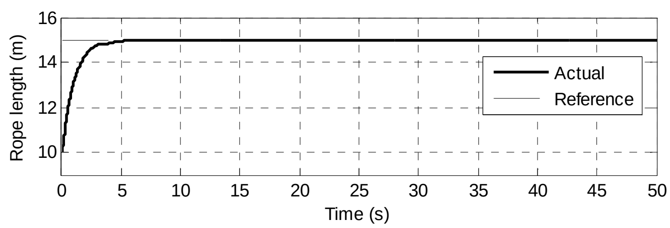

(c)

Figure 4 – (a) Luff angle; (b) swing angle; and (c) rope length; when z = 0.02 sin 1.25t m and ψ = 0.01 sin 1.25t rad.

To demonstrate the robustness of the controller, the payload is varied between 10×10^3 and 30×10^3 kg as shown in Figure 5(d). It is shown that the luff angle, the swing angle and the rope length responses are unperturbed by the presence of payload variation, which is similar with Figure 4.

CONCLUSION

In this paper we have proposed second-order sliding mode control schemes for trajectory tracking control and sway suppression for an offshore boom crane system. The offshore crane model which consists of a boom crane and a ship vessel has been simplified in order to study the effects heaving and rolling of the vessel. From a chosen sliding surface vector, a second-order sliding mode control law has been proposed, and the asymptotic stability of the closed-loop system in the Lyapunov sense has been presented. High performance in trajectory tracking and swing angle suppression are obtained either when the vessel is stationary or navigating with heave and roll motion. Robust control performance is also obtained when the system is subject to system disturbances and payload variations. Simulation results are provided to indicate the effectiveness of the proposed method.

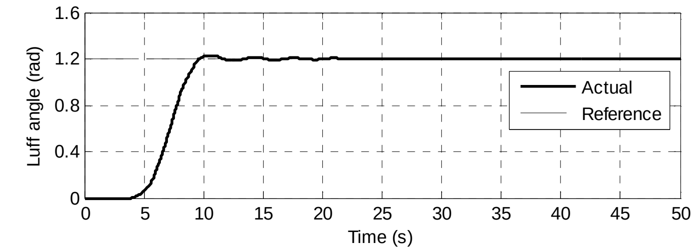

(a)

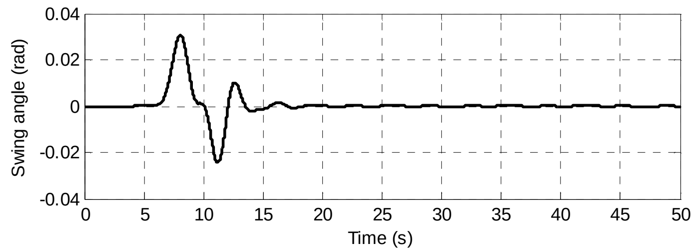

(b)

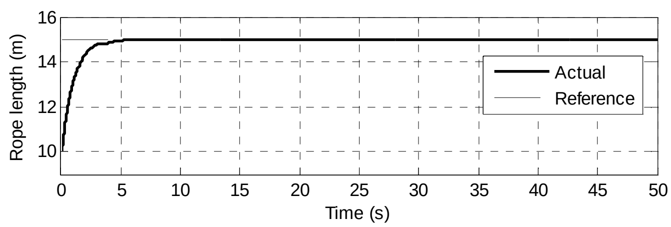

(c)

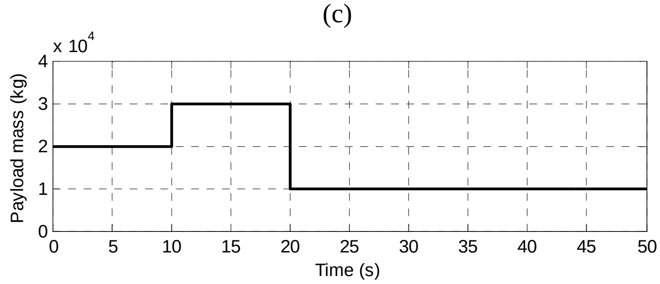

(d)

Figure 5 – (a) Luff angle; (b) swing angle; and (c) rope length; and (d) payload mass; when z = 0.02 sin 1.25t m, ψ = 0.01 sin 1.25t rad, and varying payload.

REFERENCES

Ashrafiuon, H., Muske, K.R., McNinch, L.C., & Soltan, R.A. (2008). Sliding-Mode Tracking Control of Surface Vessels," *IEEE Trans. Industrial Electronics*, 55(11):4004-4012.

Bartolini, G., Pisano, P. & Usai, E. (2002). Second-order sliding-mode control of container cranes, *Automatica*, 38(10):1783-1790.

Boiko, I., Fridman, L., & Castellanos, M. I. (2004). Analysis of Second-Order Sliding-Mode Algorithms in the Frequency Domain. *IEEE Trans. Automatic Control*, 49(6):946–950.

Fahimi, F. (2007). Sliding-Mode Formation Control for Underactuated Surface Vessels, *IEEE Trans. Robotics*, 23(3):617-622.

Fan, L., Wilson, W. W., & Dahl, B. (2012). Congestion, port expansion and spatial competition for US container imports. *Transportation Research Part E: Logistics and Transportation Review*, 48(6):1121–1136.

Fang, Y. & Wang, P. (2012). Advanced nonlinear control of an offshore boom crane. *Proc. American Control Conference*, pp. 5421-5426.

González, M. M. & Trujillo, L. (2008). Reforms and infrastructure efficiency in Spain's container ports, *Transportation Research Part A: Policy and Practice*, 42(1):243-257.

Goodchild, A.V. & Daganzo, C.F. (2007). Crane double cycling in container ports: Planning methods and evaluation, *Transportation Research Part B: Methodological*, 41(8):875-891.

Küchler, S., Mahl, T., Neupert, J., Schneider, K., & Sawodny, O. (2011). Active control for an offshore crane using prediction of the vessel's motion. *IEEE/ASME Trans. Mechatronics*, 16(2):297-309.

Levant, A. (2007). Principles of 2-sliding mode design. *Automatica*, 43(4):576-586.

Low, J. M.W., Lam, S. W., & Tang, L. C. (2009). Assessment of hub status among Asian ports from a network perspective, *Transportation Research Part A: Policy and Practice*, 43(6):593-606.

Messineo, S & Serrani, A. (2009). Offshore crane control based on adaptive external models. *Automatica*, 45(11):2546-2556.

Neupert, J., Hildebrandt, A., Sawodny, O., & Schneider, K. (2006). Trajectory Tracking For Boom Cranes Using A Flatness Based Approach, *Proc. Int. Joint Conf. SICE-ICASE*, pp. 1812-1816.

Ngo, Q. H. & Hong, K. (2012). Sliding-mode antisway control of an offshore container crane. *IEEE/ASME Trans. Mechatronics*, 17(2):201-209.

Pisano, A. & Usai, E. (2011). Sliding mode control: A survey with applications in math. *J. Mathematics and Computers in Simulation*, 81(5):954–979.

Raja Ismail, R.M.T., Nguyen, D.T., & Ha, Q.P. (2012). Observer-based trajectory tracking for a class of underactuated Lagrangian systems using higher-order sliding modes, *Proc. IEEE Int. Conf. Automation Science and Engineering*, pp. 1200-1205.

Raja Ismail, R.M.T. & Ha, Q. P. (2012). Second-order sliding mode control for offshore container crane, *Proc. Australasian Conf. on Robotics and Automation*, available online: http://www.araa.asn.au/acra/acra2012/papers/pap146.pdf.

Skaare, B. & Egeland, O. (2006). Parallel force/position crane control in marine operations. *IEEE J. Oceanic Engineering*, 31(3):599-613.

Yin, X. F., Khoo, L. P., & Chen, C.-H. (2011). A distributed agent system for port planning and scheduling. *J. Advanced Engineering Informatics*, 25(3):403-412.

Yu, R., Zhu, Q., Xia, G., & Liu, Z. (2012). Sliding mode tracking control of an underactuated surface vessel, *IET Control Theory & Applications*, 6(3):461-466.